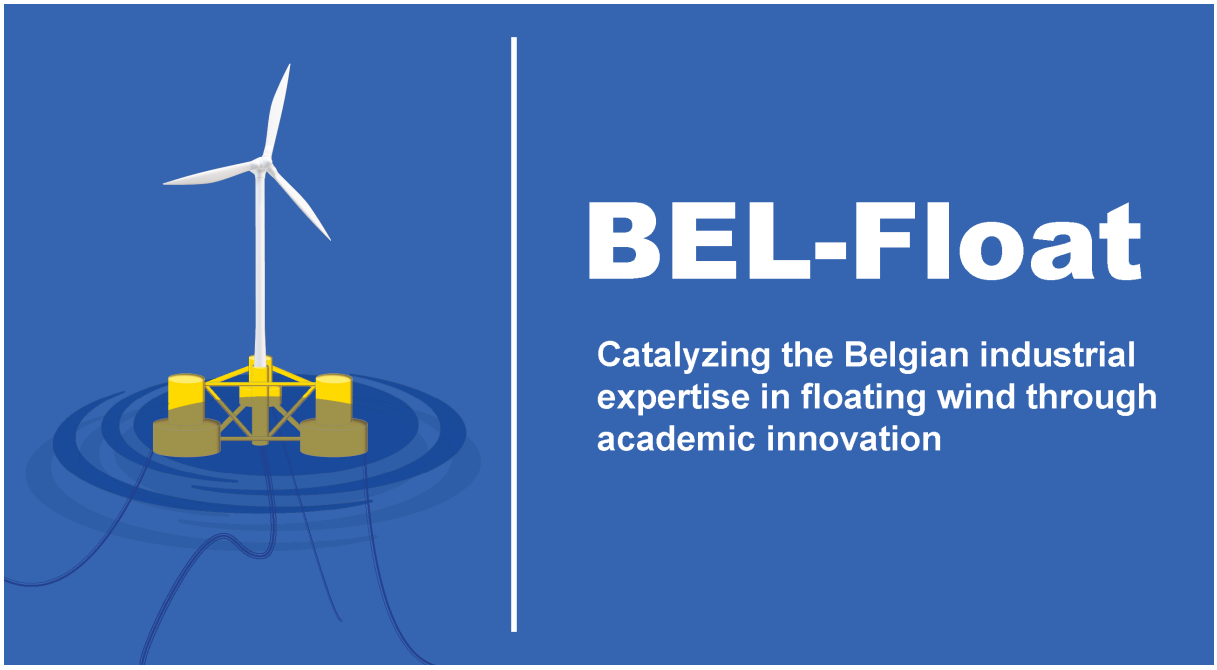

BEL-Float

Topic 3 - Low frequency dynamics of a floating platform

Benchmark study of NEMOH vs WAMIT for the OC4-DeepCwind semi-submersible FOWT

Date of delivery: 25/08/2025

Author: Abdulelah Al-Ghuwaidi
University: Vrije Universiteit Brussel

Faculty: Faculty of Engineering

Department: Department of Mechanical Engineering

Research Group: Offshore Wind Infrastructure Application Lab - OWI-Lab

Financially supported by the FPS Economy (FOD Economie) under the call 2022 of the Energy Transition Fund.

Contents

1 Introduction

This report presents a benchmark study comparing two potential-flow Boundary Element Method (BEM) panel solvers, NEMOH and WAMIT, for the OC4-DeepCwind semi-submersible platform. The hydrodynamic analysis was conducted using NEMOH and benchmarked against the published WAMIT data for the OC4 test case available from the OpenFAST [1] repository and reported in [2].

NEMOH is an open-source BEM code developed to compute wave loads on offshore structures, including added mass, radiation damping, and diffraction forces [3]. Notably, NEMOH is the only open-source solver that offers second-order solutions, which makes it suitable for this study.

The primary motivation for this work is to integrate an open-source BEM solver like NEMOH with OpenFAST for time-domain simulations under combined wave and wind conditions. The WAMIT OC4 hydrodynamic data include first-order results across different wave headings, while the second-order forces are only available for head seas (0 degrees). Therefore, this study aims to provide a complete hydrodynamic solution, including first- and second-order data for a range of wave headings from 0 to 180 degrees, leveraging NEMOH.

2 Executive Summary

The comparison results show good overall agreement between NEMOH and the WAMIT reference data for the 0 wave heading. The first-order added mass and radiation damping terms closely match, with minor discrepancies in heave, pitch, and roll, likely due to mesh resolution differences. Some high-frequency peaks were observed with NEMOH solution as shown in Figure 2.

The first-order excitation forces also showed strong agreement, with NEMOH exhibiting minor differences at peak and high-frequency regions, Figure 3. Similarly, the impulse response functions (IRFs) are consistent between both solvers, Figure 4.

The second-order solution followed the overall trends seen in WAMIT but showed greater deviations compared to the first-order data as shown in Figures 5, 6, 7. At certain frequencies, NEMOH underestimates or overestimates the WAMIT results.

The time-domain simulations using both NEMOH and WAMIT showed good agreement in free decay and under regular wave loading. The results were compared in terms of surge, heave, pitch motions, and the fairlead tension of mooring line 2. The inclusion of second-order loads (QTFs) had a significant impact on the floater motions—particularly surge (Figure 9)—and on mooring line tension (Figure 12) for shorter wave periods (T = 5 s).

3 Results

Figure 1 shows the two meshes used to generate the potential flow solutions. NEMOH (v3.0) could not process the WAMIT mesh due to its high panel density. Therefore, an alternative mesh was created using Rhino 3D [4].

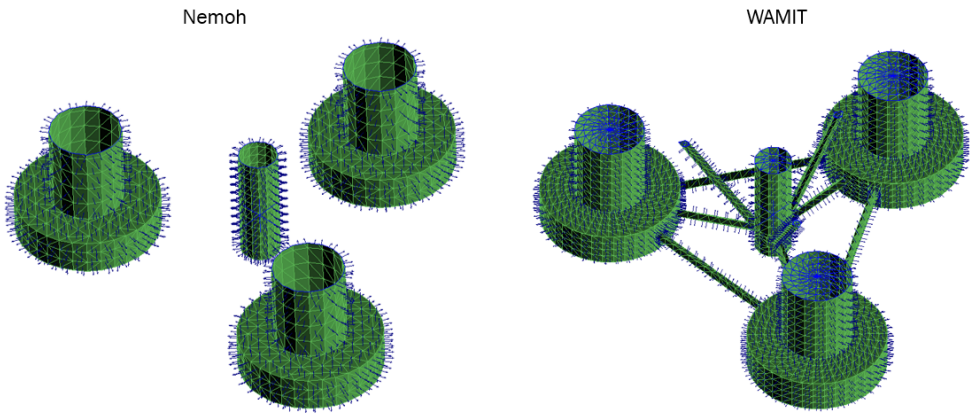

Figure 1: 3D model mesh: NEMOH vs WAMIT.

Table 1 provides a comparison of the two mesh configurations. They differ in displacement, volume, and waterplane area due to mesh resolution and the inclusion of braces in WAMIT. BEMRosetta [5] was used for preprocessing and comparison.

Table 1: Mesh Settings Comparison: NEMOH vs. WAMIT

Parameter	NEMOH	WAMIT
Number of frequencies	498	498
Min. frequency (rad/s)	0.01	0.01
Max. frequency (rad/s)	4.98	4.98
Wave directions (deg)	0	0
Mesh type	Coarse	Fine
Braces	No	Yes
No. of Panels	2,514	6,258
No. of Points	1,357	18,774
COB_z (m)	-13.2	-13.156
Displacement (kg)	13,705,968.9	14,017,733.9
Volume (m^3)	13,371.68	13,675.84
Waterplane Area (m^2)	362.94	375.29

3.1 Hydrostatic Stiffness

The hydrostatic stiffness matrices computed by both BEM solvers are shown below. WAMIT results were extracted from the ".hst" file. The relative error in heave, roll, and pitch is approximately 5%, attributed to differences in waterplane area, volume, and mesh characteristics.

$$\text{WAMIT} = \begin{bmatrix} 0 & 0 & 0 & 0 & 0 & 0 \\ 0 & 0 & 0 & 0 & 0 & 0 \\ 0 & 0 & 380.0615 & 0 & -0.01533 & 0 \\ 0 & 0 & 0 & -37875.5 & 0 & 0 \\ 0 & 0 & -0.01533 & 0 & -37875.27 & 0 \\ 0 & 0 & 0 & 0 & 0 & 0 \end{bmatrix}$$

$$\text{NEMOH} = \begin{bmatrix} 0 & 0 & 0 & 0 & 0 & 0 \\ 0 & 0 & 0 & 0 & 0 & 0 \\ 0 & 0 & 362.9425 & -0.00398 & 0.9356 & 0 \\ 0 & 0 & -0.00398 & -35892.95 & 0 & 0 \\ 0 & 0 & 0.9356 & 0 & -35909.96 & 0 \\ 0 & 0 & 0 & 0 & 0 & 0 \end{bmatrix}$$

3.2 Added Mass and Radiation Damping

Figure 2 shows the frequency-dependent added mass computed by NEMOH and compared to WAMIT. The results in general have good agreement with some differences in Heave, pitch and roll. Also there are some visible peaks with NEMOH solution at higher frequencies.

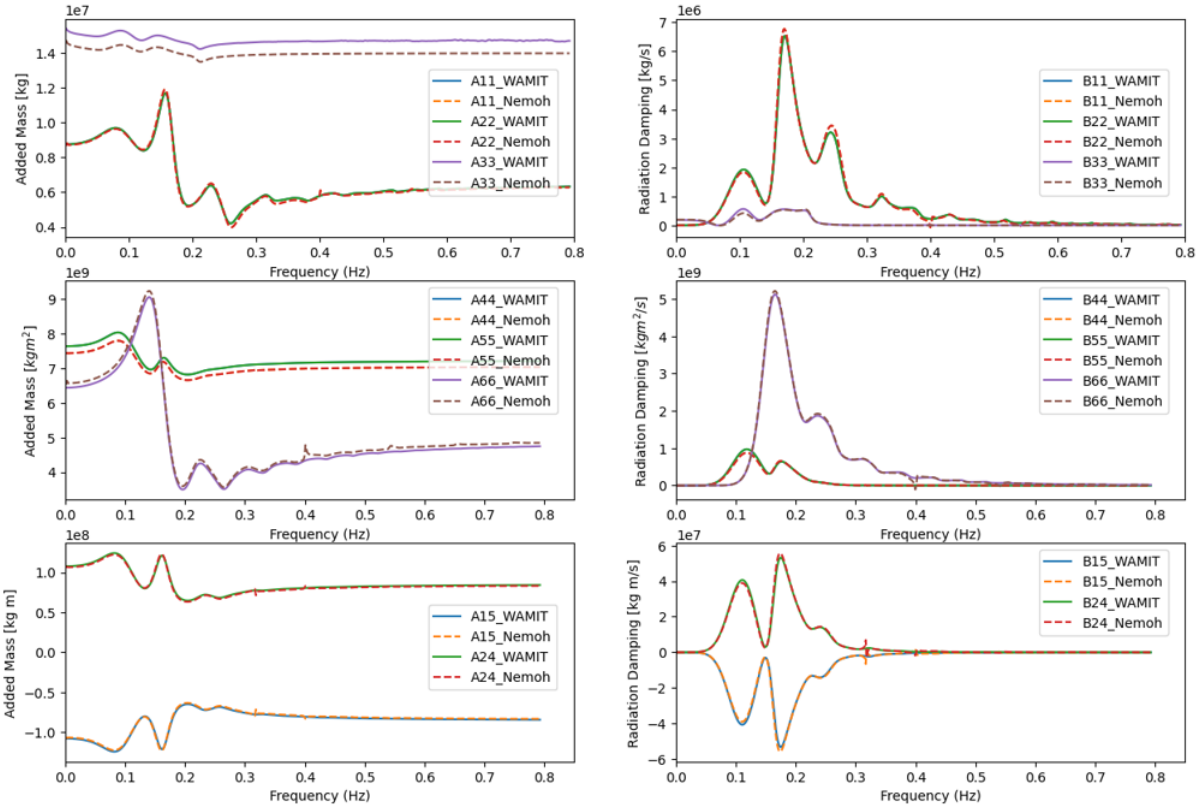

Figure 2: Added mass and radiation damping comparison: NEMOH vs. WAMIT.

3.3 First-Order Excitation Forces

Similarly, Figure 3 shows the frequency-dependent 1st order excitation loads computed by NEMOH and compared to WAMIT. The results in general have good agreement with some differences in the peaks. Additionally, there are some visible peaks with NEMOH solution at higher frequencies.

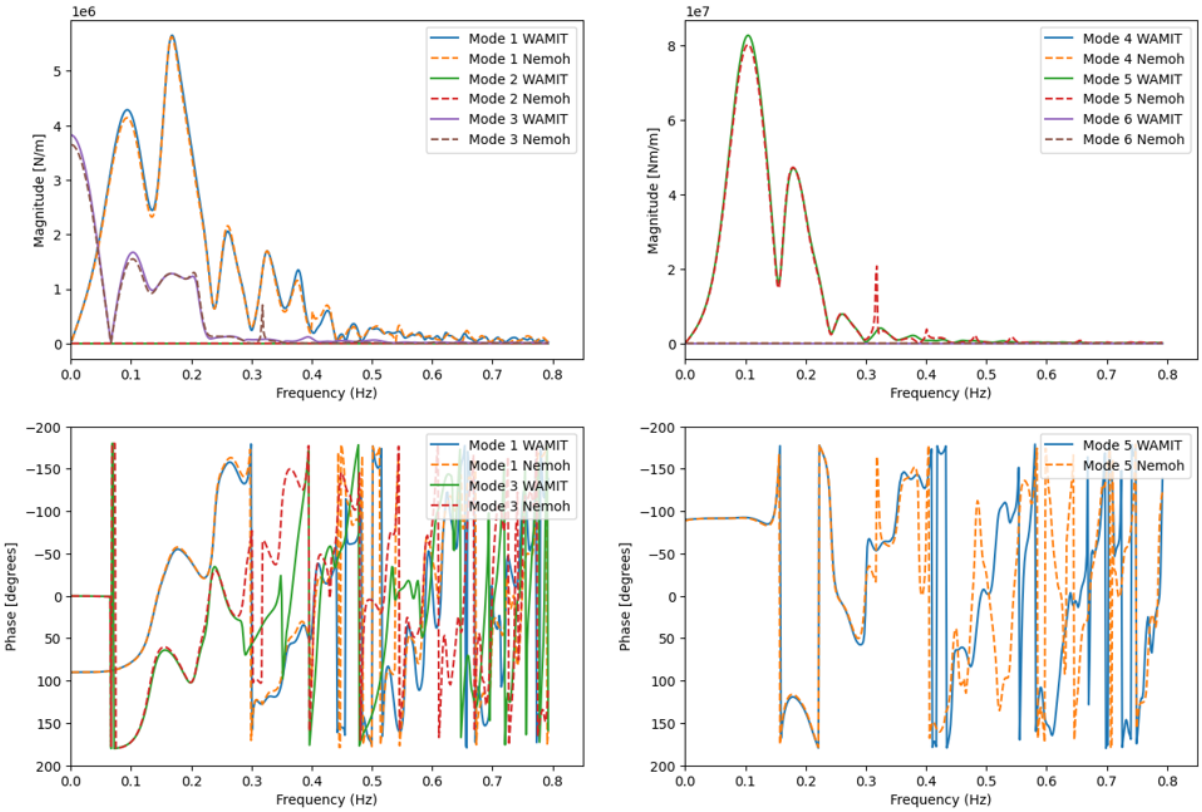

Figure 3: First-order excitation forces: NEMOH vs. WAMIT (Phase plots for Modes 2, 4, and 6 removed for clarity).

3.4 Impulse Response Functions (IRFs)

Here. the results matched well between the two BEM solvers with slight variation in some peaks as shown in Figure 4.

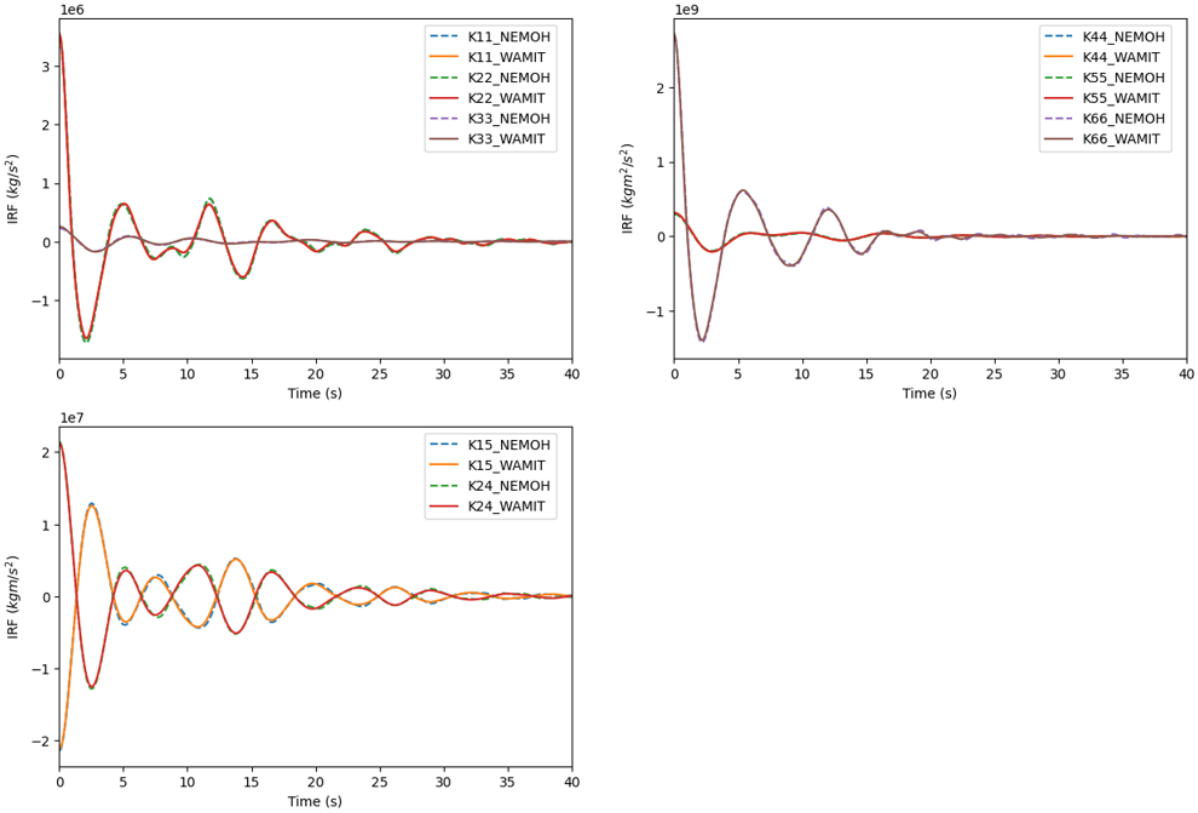

Figure 4: Impulse Response Functions (IRFs) comparison. Data extracted using BEMRosetta [5].

3.5 Second-Order Solution

3.5.1 Inertia and Mooring Stiffness

According to the HydroDyn manual, second-order analysis requires explicit definitions of the system's inertia matrix, mooring stiffness matrix, and center of gravity. The following matrices were extracted from the OpenFAST WAMIT '.frc' file provided by NREL.

$$I = \begin{bmatrix} 1.407 \times 10^7 & 0 & 0 & 0 & -1.392 \times 10^8 & 0 \\ 0 & 1.407 \times 10^7 & 0 & 1.392 \times 10^8 & 0 & -1.448 \times 10^5 \\ 0 & 0 & 1.407 \times 10^7 & 0 & 1.448 \times 10^5 & 0 \\ 0 & 1.392 \times 10^8 & 0 & 1.270 \times 10^{10} & -1.094 \times 10^{-1} & 1.167 \times 10^7 \\ -1.392 \times 10^8 & 0 & 1.448 \times 10^5 & -1.094 \times 10^{-1} & 1.269 \times 10^{10} & -1.953 \\ 0 & -1.448 \times 10^5 & 0 & 1.167 \times 10^7 & -1.953 & 1.229 \times 10^{10} \end{bmatrix}$$

$$K_{\text{mooring}} = \begin{bmatrix} 7.084 \times 10^4 & 0 & 0 & 0 & -1.080 \times 10^5 & 0 \\ 0 & 7.084 \times 10^4 & 0 & 1.080 \times 10^5 & 0 & 0 \\ 0 & 0 & 1.910 \times 10^4 & 0 & 0 & 0 \\ 0 & 1.070 \times 10^5 & 0 & 8.730 \times 10^7 & 0 & 0 \\ -1.070 \times 10^5 & 0 & 0 & 0 & 8.730 \times 10^7 & 0 \\ 0 & 0 & 0 & 0 & 0 & 1.170 \times 10^8 \end{bmatrix}$$

3.5.2 Quadratic Transfer Functions (QTFs)

Figure 5 shows the second-order difference-frequency results for surge. The mean drift load is shown in the right plot between NEMOH and WAMIT by taking the diagonal terms shown by the red diagonal line in the left and mid plots. Results of WAMIT in the mid figure was mirrored due to symmetry of the OC4 platform since only half of the data was available in the .12d and 12.s files. Good agreement between the two BEM solvers at lower frequencies compared to higher frequencies where some variation is observed.

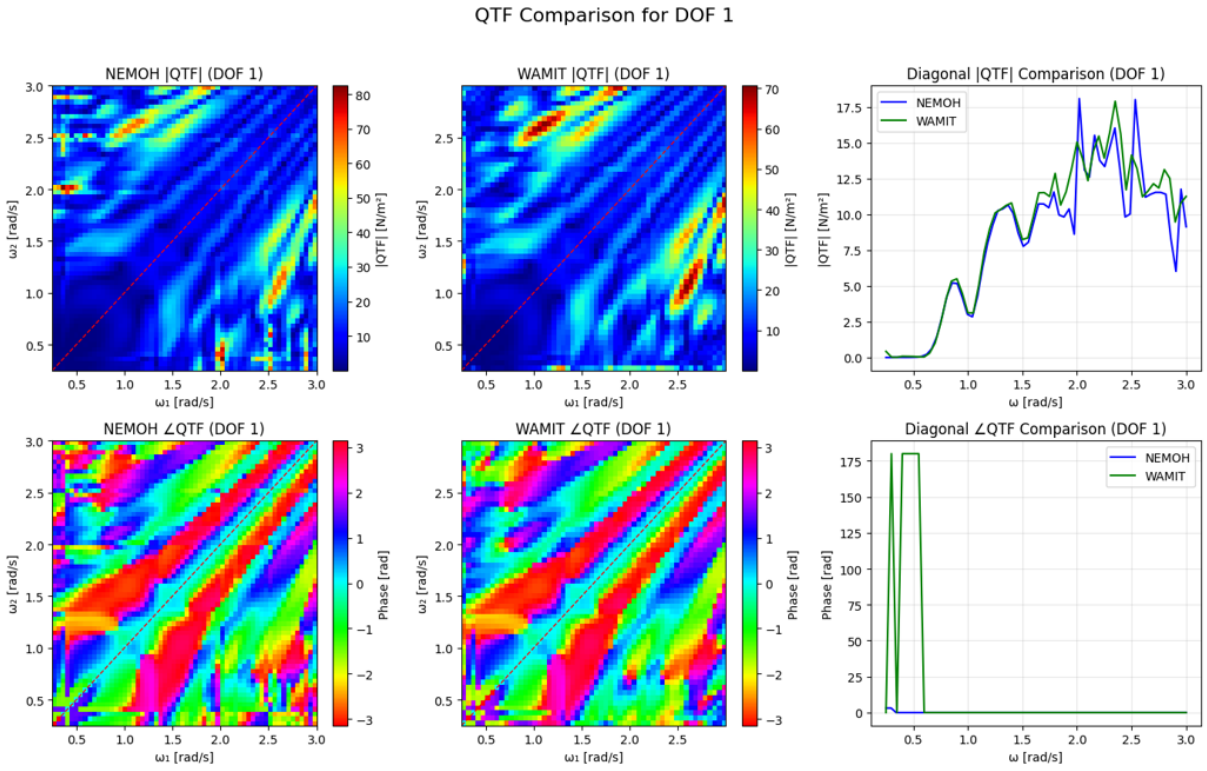

Figure 5: QTF Difference-Frequency for surge at 0 wave direction: NEMOH vs. WAMIT (WAMIT mirrored).

Figure 6 shows the second-order difference-frequency results for heave. The mean drift load is shown in the right plot between NEMOH and WAMIT by taking the diagonal terms shown by the red diagonal line in the left and mid plots. In contrast to surge, good agreement between the two BEM solvers at higher frequencies compared to lower frequencies where NEMOH solution underestimated WAMIT. Figure 7 shows the second-order difference-frequency results for pitch. While the general behavior is captured by the two BEM solutions, there are more variations particularly for peak loads.

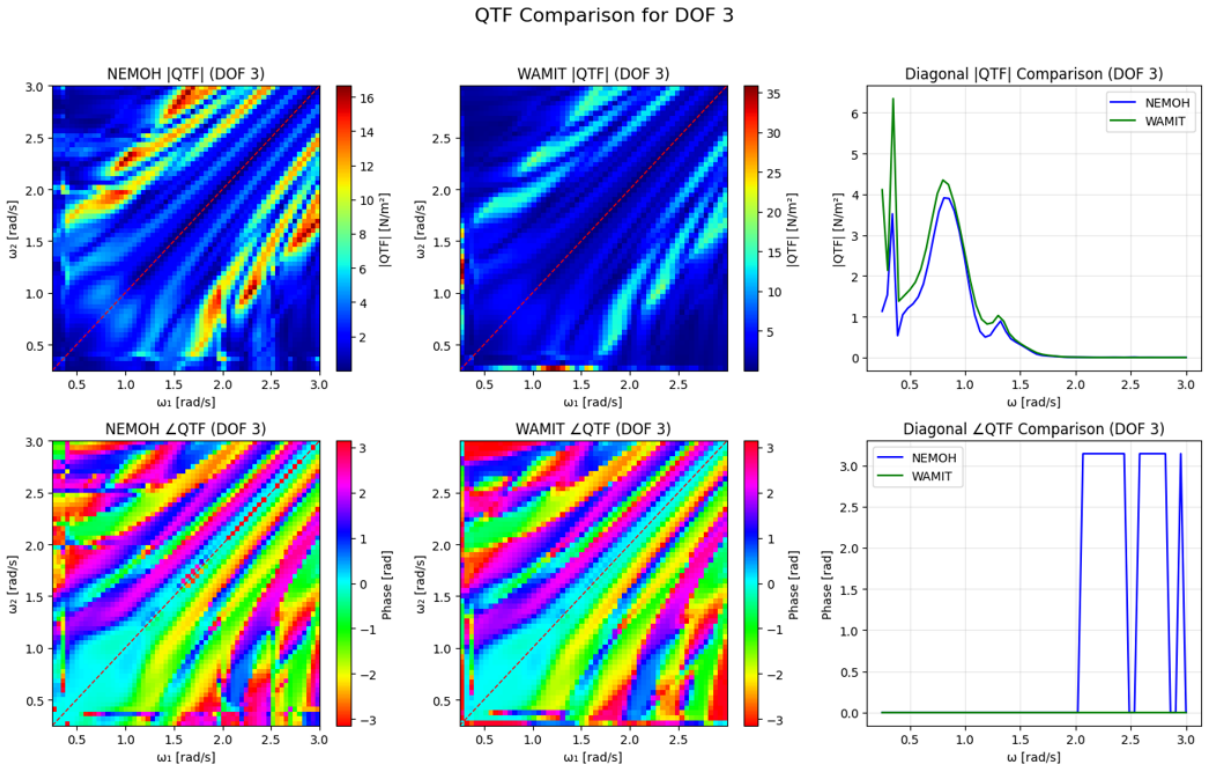

Figure 6: QTF Difference-Frequency for heave at 0 wave direction: NEMOH vs. WAMIT (WAMIT mirrored).

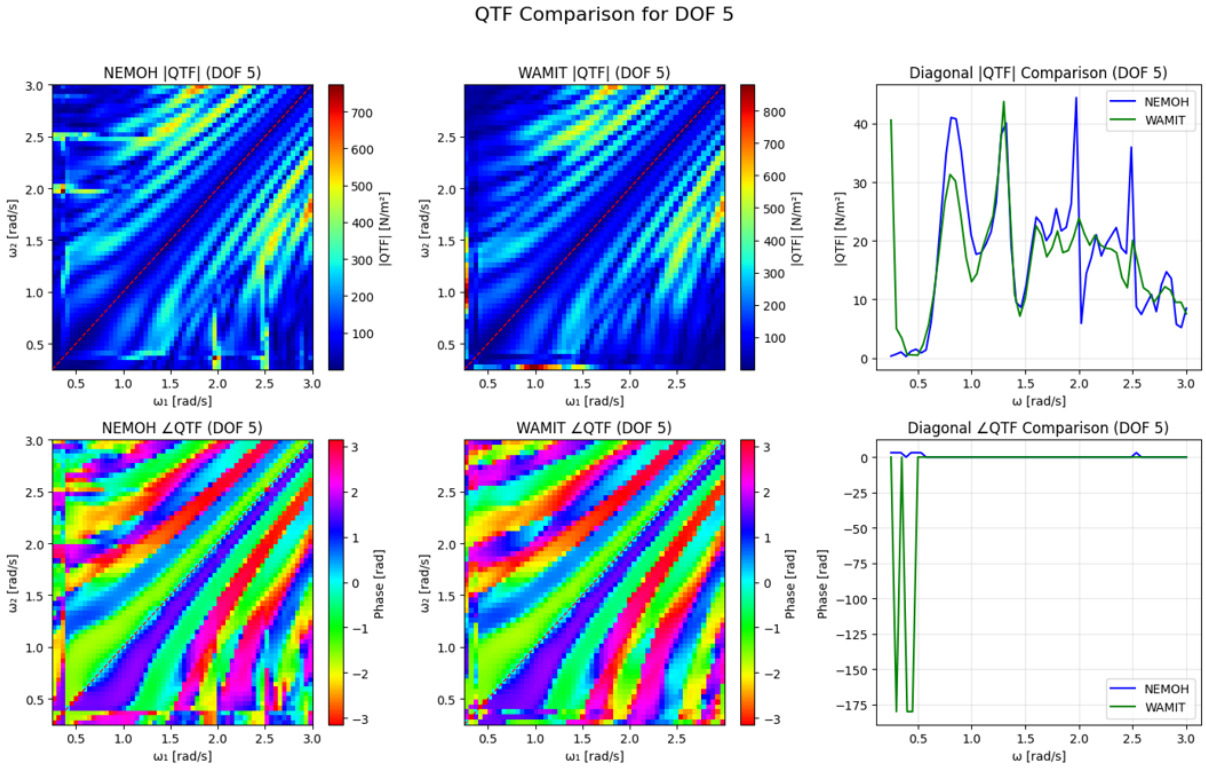

Figure 7: QTF Difference-Frequency for pitch at 0 wave direction: NEMOH vs. WAMIT (WAMIT mirrored).

3.6 Time-domain simulation

Selected cases were simulated in OpenFAST using the hydrodynamic solution generated by NEMOH and compared with the available WAMIT solution. The NEMOH solution was first converted into WAMIT format using BEMRosetta [5], since this format is compatible with OpenFAST.

3.6.1 Free Decay

Figure 8 presents the results of free-decay tests in OpenFAST using the NEMOH solution, compared with WAMIT. In general, good agreement is observed between the two BEM solvers, with minor differences in pitch and heave due to variations in the hydrostatic matrix.

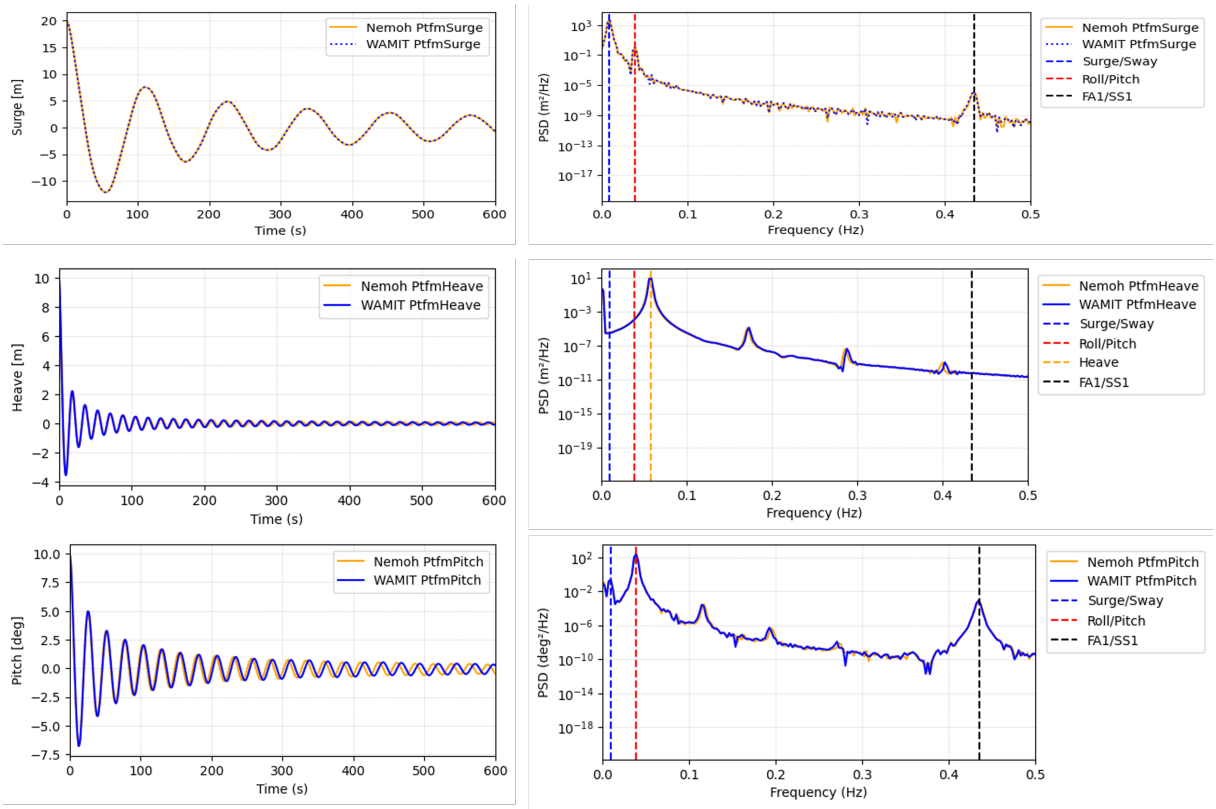

Figure 8: Free-decay simulations in OpenFAST for surge, heave, and pitch. The vertical dashed line represents the design natural frequencies obtained from the eigenvalue solution.

3.6.2 Regular Waves

The OC4 FOWT was subjected to different load cases (LCs) with a fixed wave height and varying wave periods. As shown in Figure 9, both NEMOH and WAMIT solutions matched well for the selected regular-wave cases. The load case with $H = 5$ m and $T = 5$ s highlights the effect of second-order (QTF) forces on the surge response of the OC4 platform.

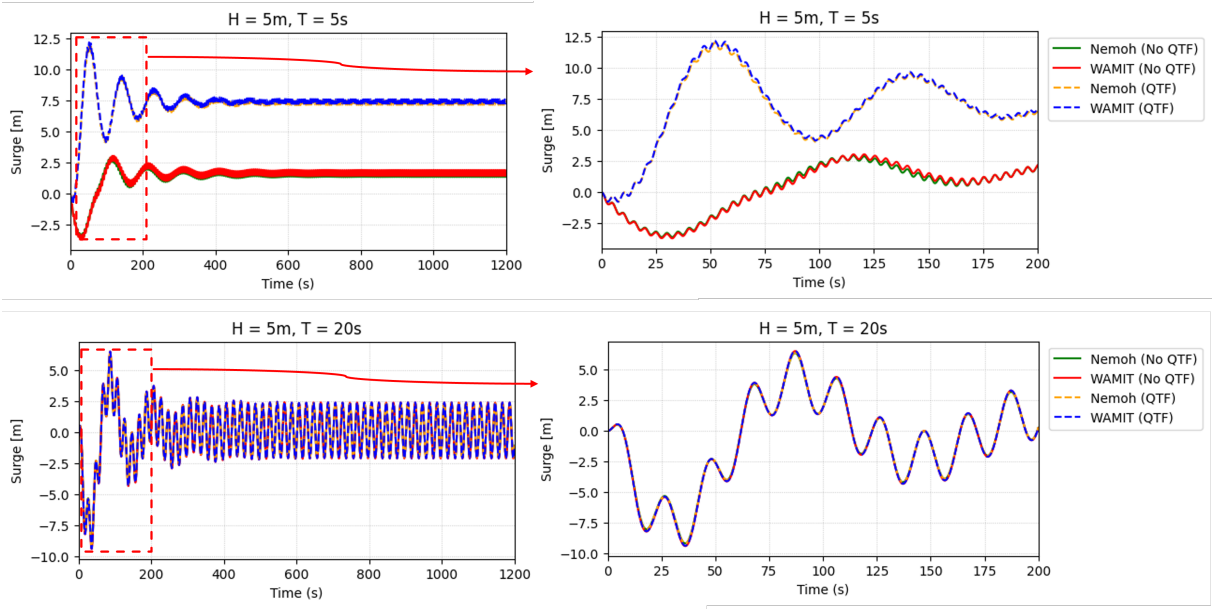

Figure 9: Surge response to two regular waves.

Figure 10 shows the heave response for two regular waves ($H = 5$ m, $T = 5$ s and $T = 20$ s). The influence of second-order forces is less significant in heave compared to surge for the selected cases. The heave amplitude is larger for $T = 20$ s compared to $T = 5$ s, since the longer period is closer to the natural heave frequency (around 17 s). Overall, the NEMOH results agreed well with the WAMIT solution, with only minor variations in amplitude.

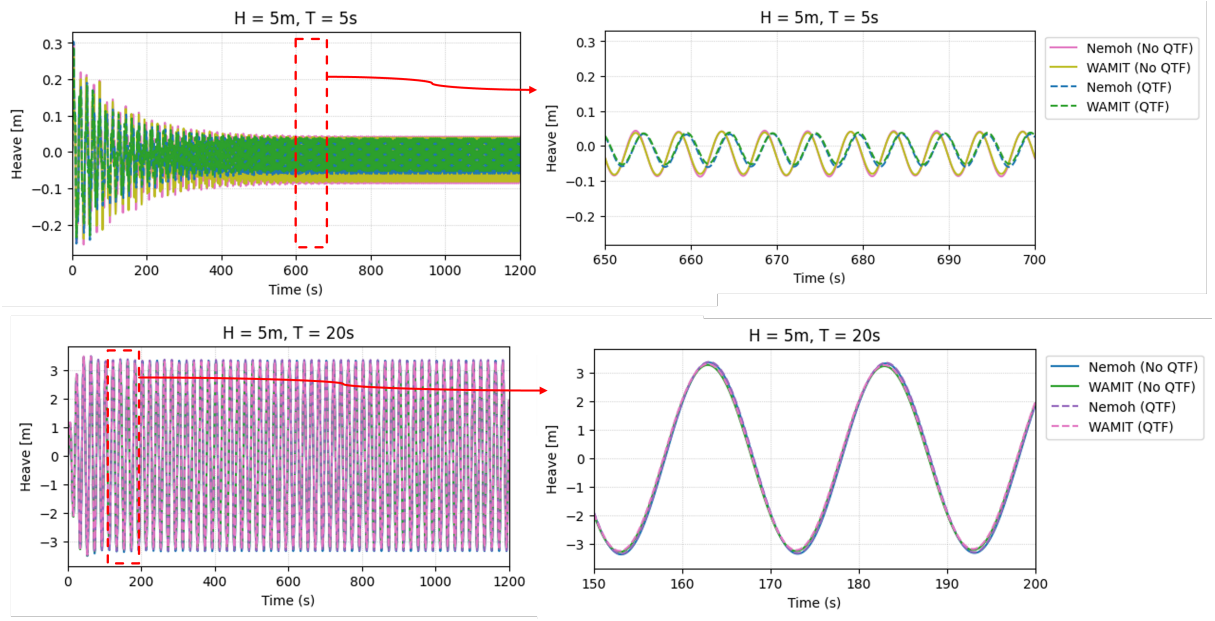

Figure 10: Heave response to two regular waves.

The pitch response to the selected regular waves ($H = 5$ m, $T = 5$ s and $T = 20$ s) is shown in Figure 11. Similar to surge, the effect of second-order forces is visible in the pitch response for shorter wave periods. As shown, there are some differences in phase and amplitude between NEMOH and WAMIT. However, these differences remain limited.

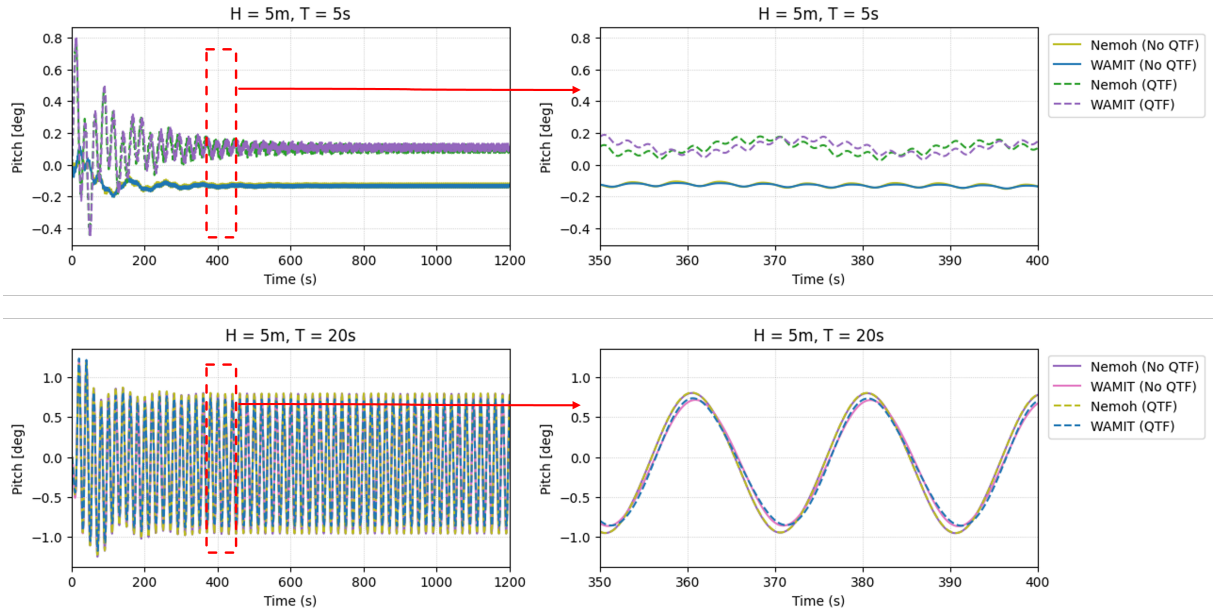

Figure 11: Pitch response to two regular waves.

Finally, the mooring-line tension at the fairlead of line 2 is compared in Figure 12. The second-order forces significantly influenced the mooring-line tension for short-period waves ($T = 5$ s). For longer waves, however, the impact of including QTFs was limited. In both cases, the NEMOH solution matched the WAMIT results closely.

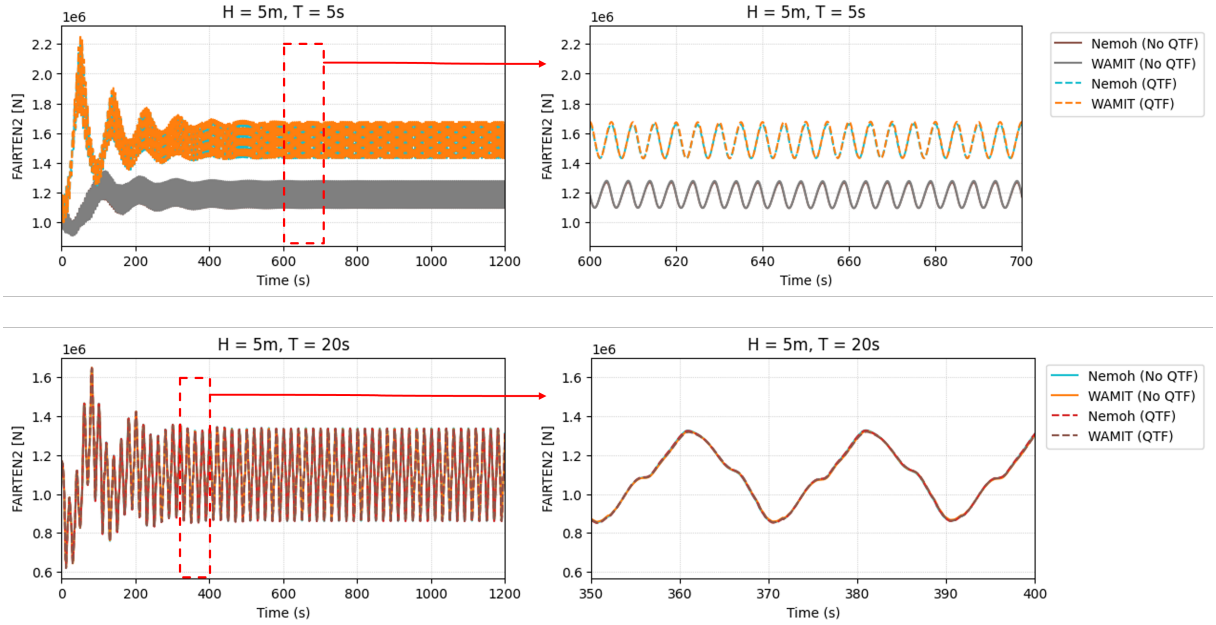

Figure 12: Mooring-line tension at the fairlead of line 2 under two regular waves.

4 Conclusion and Future work

This study benchmarked NEMOH against WAMIT for the OC4-DeepCwind semi-submersible. First-order results (added mass, radiation damping, excitation forces, and IRFs) showed good agreement, with minor differences attributed to mesh resolution and geometry. Second-order results followed the same overall trends but exhibited larger deviations at certain frequencies. Time-domain simulations in OpenFAST confirmed the reliability of NEMOH, with second-order forces significantly influencing surge and mooring tension in short-period waves.

Future work will focus on extending the comparison to irregular seas, refining the mesh to better capture hydrodynamic coefficients, and improving integration with OpenFAST via formats conversion specifically for the QTF results with multiple wave headings to enable streamlined use of NEMOH for coupled offshore wind simulations. Also, studying in depth the reason behind the variation in QTF results.

References

[1] N. R. E. L. (NREL), "Openfast: An open-source wind turbine simulation tool," 2024.

[2] A. Robertson, J. Jonkman, A. Goupee, A. Coulling, and C. Luan, "Definition of the semisubmersible floating system for phase ii of oc4," 2014.

[3] L. Lab, "Nemoh: A hydrodynamics code based on the linear potential flow theory." `https://gitlab.com/lheea/Nemoh`, 2025. Accessed: 2025-08-05.

[4] Robert McNeel & Associates, *Rhinoceros 3D*. Robert McNeel & Associates, Seattle, USA, 2025. Version 8.0.

[5] R. L. Boulluec and C. Ducros, "Bemrosetta: A bem data converter and post-processing tool." `https://github.com/LHEEA/BEMRosetta`, 2020. Accessed: 2025-08-05.